

# Angular distribution of reactive carbon dioxide desorption on a rhodium (110) surface

Tatsuo Matsushima and Yuichi Ohno

*Catalysis Research Center, Hokkaido University, Sapporo 060, Japan*

Received 18 March 1993; accepted 17 September 1993

The angular distribution of reactive CO<sub>2</sub> desorption was studied on Rh(110) by means of angle-resolved thermal desorption. Four CO<sub>2</sub> formation peaks appear in the range of 170–500 K. The distribution of the desorption collimated along the surface normal becomes sharp with increasing reactant coverages. No azimuth dependence is found in the distribution.

**Keywords:** Angular distribution; CO<sub>2</sub> desorption; rhodium(110)

## 1. Introduction

The identification of reaction sites is one of the most important pieces of information for understanding chemical reactions sensitive to the surface structure. The structural information of reaction sites cannot be obtained from spectroscopic analysis of non-reacting surface species. It can be provided only through the reaction dynamics. The angular distribution of the product desorption provides this structural information, when the molecules are repulsively desorbed. The reactive CO<sub>2</sub> desorption is one of typical processes of this kind. The distribution depends on the density of reactants, and on the symmetry and orientation of the reaction site [1–4]. This symmetry is useful for the identification of the reaction site. Anisotropic vibrational motions are expected for the product molecules parallel to the surface plane immediately before the desorption, when the reaction site is in a highly asymmetric structure. Such motion yields anisotropic angular distribution, as frequently observed in electron stimulated desorption ion distribution (ESDIAD) [5]. In fact, the anisotropy is found in the reactive CO<sub>2</sub> desorption on Pd(110) [2]. It is correlated with the symmetry of the reaction site in the surface trough. A similar anisotropy is expected in the reactive CO<sub>2</sub> desorption on Rh(110), since this surface has troughs extended in the  $[\bar{1}10]$  direction and it has been proposed that oxygen be located in the trough [6,7]. This paper reports the angular distribution of reactive CO<sub>2</sub> desorption on this surface. The distribution becomes sharp as the reactant

coverage increases. Restructuring of the surface is proposed, since no crystal azimuth dependence is found in the distribution in contrast to the above prediction.

## 2. Experimental

The experimental apparatus was reported previously [4]. It consists of a reaction chamber with LEED-AES, an analyzer chamber and a collimator. CO<sub>2</sub> molecules desorbing from the surface and passing the slits of the collimator contribute to the signal of the mass spectrometer in the analyzer chamber, yielding angle-resolved spectra. The desorption is also recorded in the angle-integrated form with another mass spectrometer in the reaction chamber. A rhodium crystal (10 mm diameter  $\times$  1 mm thick) was mounted on a holder that allowed rotation of the crystal azimuth,  $\phi$ , and also the desorption angle,  $\theta$  (the polar angle). It is cooled to 133 K and heated resistively. It was cleaned by prolonged cycles of oxygen treatment at 800 K and argon ion bombardment at 1000 K. It was finally heated to 1350 K. The resultant surface showed a (1  $\times$  1) LEED pattern.

The coverages of CO and oxygen,  $\theta_{\text{CO}}$  and  $\theta_{\text{O}}$ , were determined by thermal desorption (TDS) and normalized to the value reported in the literature. They are expressed in monolayer (ML) where 1 ML = a CO molecule or an oxygen adatom per surface Pt atom. The saturation coverage is 1.0 for oxygen [7], and also for CO [8].

## 3. Results and discussion

### 3.1. CO<sub>2</sub> FORMATION

CO<sub>2</sub> formation spectra were recorded as follows. The clean surface was first exposed to <sup>18</sup>O<sub>2</sub> up to a desired  $\theta_{\text{O}}$  value at 190 K. No molecular desorption is found at this temperature. The surface was further exposed to C<sup>16</sup>O in various amounts at 150 K. The surface was heated at a rate of 22–24 K/s. A series of typical CO<sub>2</sub> formation spectra in both forms is shown in fig. 1, where the surface precov-  
ered by oxygen at  $\theta_{\text{O}} = 0.40$  was exposed to CO in various amounts. A single peak of C<sup>16</sup>O<sup>18</sup>O formation, P<sub>1</sub>-CO<sub>2</sub>, appears around 450 K when both coverages are small. Oxygen is simply referred to as O, because only C<sup>16</sup>O<sup>18</sup>O is produced. With increasing CO coverage, the CO<sub>2</sub> formation is extended to lower temperatures, yielding three additional CO<sub>2</sub> peaks, P<sub>2</sub>-CO<sub>2</sub> around 400 K, P<sub>3</sub>-CO<sub>2</sub> ( $\sim$  320 K) and P<sub>4</sub>-CO<sub>2</sub> ( $\sim$  200 K). When the oxygen precoverage is high, the P<sub>2</sub>-CO<sub>2</sub> peak first appears even at small CO coverages, as shown in the figure.

Several such peaks are frequently observed in the thermal CO<sub>2</sub> formation spectra on platinum metals. The coadsorption of CO and oxygen on these metal surfaces is characteristic of the separate domains of each species [1,2,9–11]. The

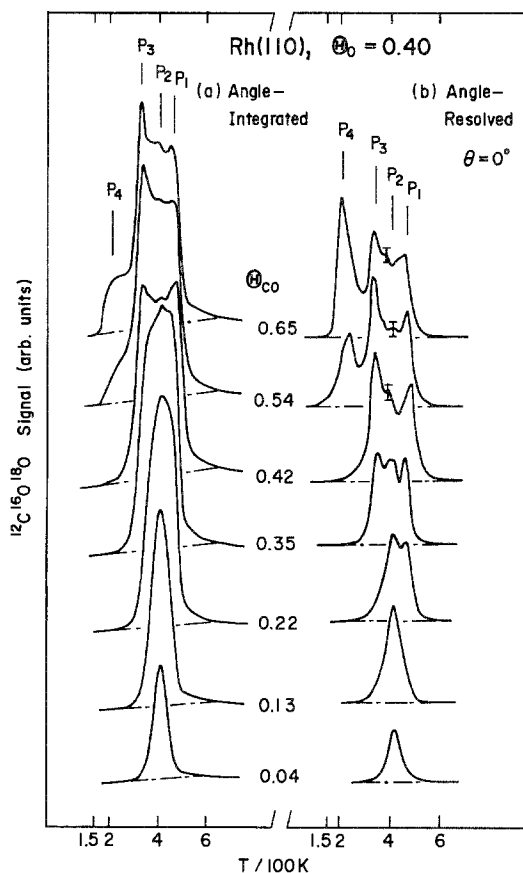


Fig. 1. CO<sub>2</sub> formation spectra generated at various CO coverages and a high oxygen coverage in (a) angle-integrated and (b) angle-resolved form observed at the surface normal. The vertical bars indicate typical noise levels. The heating rate is 22 K/s.

domains are compressed into lattices with higher densities, when the coverages exceed threshold values. The activation energy for the CO<sub>2</sub> formation is reduced on the perimeters of the compressed lattices, since the heat of adsorption of the reactants is decreased. This causes additional CO<sub>2</sub> formation peaks at lower temperatures in TDS spectra. In the present experiments, the threshold coverages for the P<sub>4</sub>-CO<sub>2</sub> formation were determined by monitoring the appearance of this signal in the angle-resolved form in the normal direction, since the angular distribution collimated along the surface normal becomes sharp with increasing coverage, as shown below. The appearance of the CO<sub>2</sub> peak at higher coverages is sensitively found in the normal direction. It has been confirmed that the P<sub>4</sub>-CO<sub>2</sub> peak appears as the coverages exceed the relation of  $\theta_{\text{CO}}/0.75 + \theta_{\text{O}}/0.8 \approx 1$ . Here, each coefficient involves about 10% experimental errors. This relation indicates that P<sub>4</sub>-CO<sub>2</sub> appears when the local coverage of CO is above 0.75 or that of oxygen above 0.80.

Oxygen forms six super-lattices;  $p(2 \times 3)(\Theta_{\text{O}} = 0.3)$ ,  $np(2 \times 2)(0.5)$ ,  $np(2 \times 3)(0.65)$ ,  $c(2 \times 6)(0.8)$ ,  $c(2 \times 8)(0.85)$  and  $c(2 \times 10)(0.9)$  [7]. On the other hand, CO yields two lattices,  $c(2 \times 2)(\Theta_{\text{CO}} = 0.5)$  and  $(4 \times 2)(0.75)$ . Here, several coadsorption structures consisting of separate domains may be produced. The oxygen lattices are easily compressed into the lattices with higher density. Such compression proceeds sequentially with increasing CO coverage [9–11].  $P_4\text{-CO}_2$  is likely to be formed in the coadlayer of  $c(2 \times 6)\text{-O}$  and  $(4 \times 2)\text{-CO}$  domains. Below the coverage in the above relation, the coadsorption may produce different structures yielding four  $\text{CO}_2$  formation peaks. In fact, three of them are observed experimentally. No successful analysis is obtained for the threshold coverages of the peaks, because they are severely overlapped.

### 3.2. ANGULAR DISTRIBUTION

A comparison of  $\text{CO}_2$  spectra in both angle-integrated and angle-resolved forms in fig. 1 indicates that the desorption of  $\text{CO}_2$  is collimated along the surface normal more sharply as the CO coverage increases. The ratio of the signal in the angle-resolved form to that in the angle-integrated form increases with an increase in the CO coverage. Typical angle-resolved spectra observed at various desorption angles are summarized in fig. 2b, as well as an angle-integrated spectrum observed simultaneously. The  $\text{CO}_2$  signal in the angle-integrated form is small compared with that of CO, since the pumping rate of  $\text{CO}_2$  is very high in the reaction chamber. The  $P_4\text{-CO}_2$  peak is relatively small in the angle-integrated form. On the other hand, it is enhanced in the angle-resolved form in the normal direction and decreased rapidly with increasing desorption angle. This means a sharp angular distribution of  $P_4\text{-CO}_2$ .

The angular distribution of  $P_1\text{-CO}_2$  was determined at small coverages of both reactants. On the other hand, the distribution of  $P_2\text{-CO}_2$  was determined at small CO coverages where only this  $\text{CO}_2$  is observed as shown in fig. 1. The results are shown in fig. 3. The background level observed at  $\theta = 90^\circ$  was first subtracted from the signal. The resultant signal was corrected by considering an increasing area falling into the aperture angle when the angle was shifted from the bulk surface normal. The distribution shows a  $(\cos \theta)^{3 \pm 0.5}$  dependence for  $P_2\text{-CO}_2$ . It is somewhat broader for  $P_1\text{-CO}_2$  as  $(\cos \theta)^{2 \pm 0.5}$ , and sharper for  $P_3\text{-CO}_2$  as  $(\cos \theta)^{5 \pm 1}$ . The latter was determined at high CO coverages. The angular distribution of  $P_4\text{-CO}_2$  is very sharp as  $(\cos \theta)^{12 \pm 2}$  as shown in fig. 4. The distribution is sharpened as the coverage increases. This sharpening is a common phenomenon in the reactive  $\text{CO}_2$  desorption [2,3]. The desorption is accelerated along the normal direction of the reaction site as the coverage increases, since the repulsive interaction between the adsorbates increases [2].

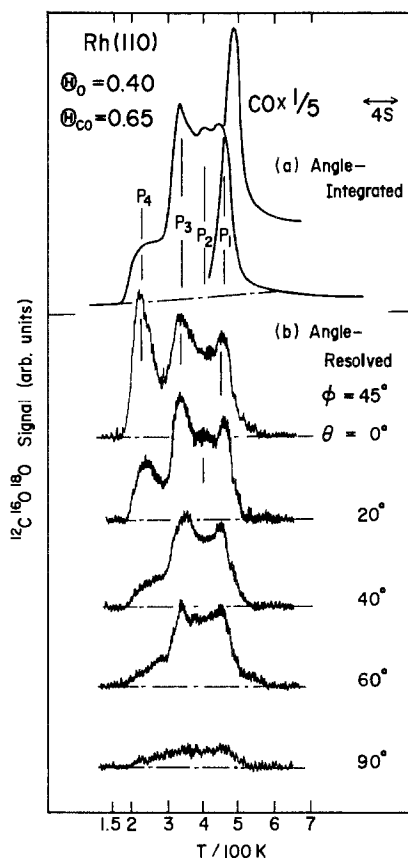


Fig. 2. (a) A CO<sub>2</sub> formation spectrum generated at a high CO coverage in angle-integrated form. (b) Angle-resolved spectra observed at various desorption angles. The azimuth is defined in fig. 3.

### 3.3. REACTION SITE

The product CO<sub>2</sub> is formed from the reaction of CO(a) with O(a). The binding energy of O(a) is high, about 95 kcal/mol [6,7]. This adatom is relatively immobile [7]. On the other hand, the activation energy for surface diffusion of CO(a) has been reported to be only 4.4 kcal/mol on Pt(111) terraces [12]. The reaction is likely to proceed on each oxygen adsorption site. It has been proposed that oxygen be located in the trough [6,7].

The anisotropy in the angular distribution of desorbing surface species has frequently been observed in ESDIAD experiments [5]. It is originated from the anisotropic shape of the potential well for the hindered translational or rotational motions of ad molecules immediately before the desorption. It is, therefore, correlated with the symmetry of the adsorption site. A similar model was used for the

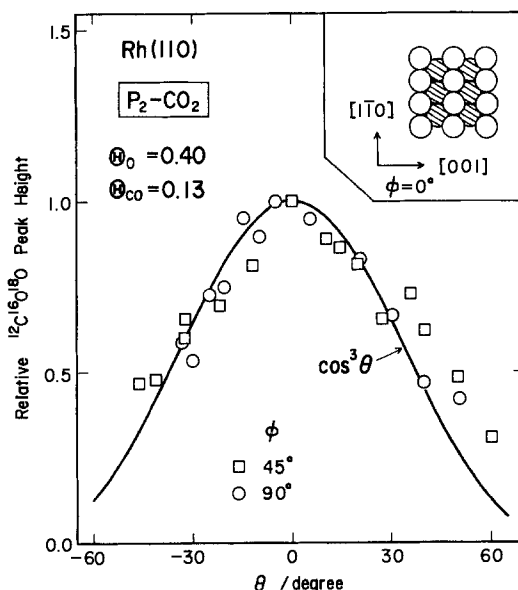


Fig. 3. Angular distribution of the  $P_2$ -CO<sub>2</sub> flux in two crystal azimuths. The crystal azimuth is defined in the inserted figure.

anisotropic angular distribution of reactive CO<sub>2</sub> desorption on Pd(110) [2], where the reaction site is located in the surface trough. The motion of CO<sub>2</sub> being produced is severely restricted by closely surrounding palladium atoms, yielding a sharper angular distribution in the [001] direction. This principle should work on the present surface, if the reaction site is in the surface trough.

However, no crystal azimuth dependence is found in the angular distribution on the present surface. The results for  $P_4$ -CO<sub>2</sub> and  $P_2$ -CO<sub>2</sub> are shown in figs. 4 and 5. The adsorption site for oxygen may be changed from the trough into the site with a higher symmetry. This is reminiscent of the adsorption structure of oxygen on Cu(110) [13,14] and Ag(110) [15] surfaces, which have been observed by scanning tunneling microscopy (STM). The structure analysis by low energy electron diffraction (LEED) first suggested that oxygen was located in the trough. However, STM shows clearly that oxygen is not in the trough. It is located in the top-most atomic row extended in the  $[1\bar{1}0]$  direction. The site in the trough, which has been considered to be occupied by oxygen, is covered by metal atoms. Surface restructuring occurs during oxygen adsorption. A metal-oxygen compound is rather stable on these surfaces and has a tendency to form one-dimensional chains extended in the [001] direction. A similar situation may be expected on Rh(110), since LEED patterns after oxygen adsorption are quite close to those on Ag, Cu(110) surfaces. No crystal azimuth dependence may be expected in the angular distribution, when CO<sub>2</sub> is produced on the top of atom row. No STM data have

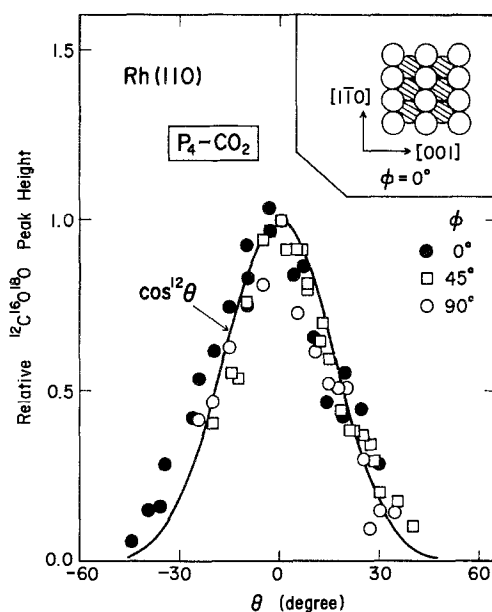


Fig. 4. Angular distribution of the  $P_4$ -CO<sub>2</sub> flux in three crystal azimuths.

been reported for oxygen-covered Rh(110). Restructuring of Rh(110) surfaces has recently been observed by LEED [6,16]. However, no structure analysis for oxygen adsorption sites has been given yet.

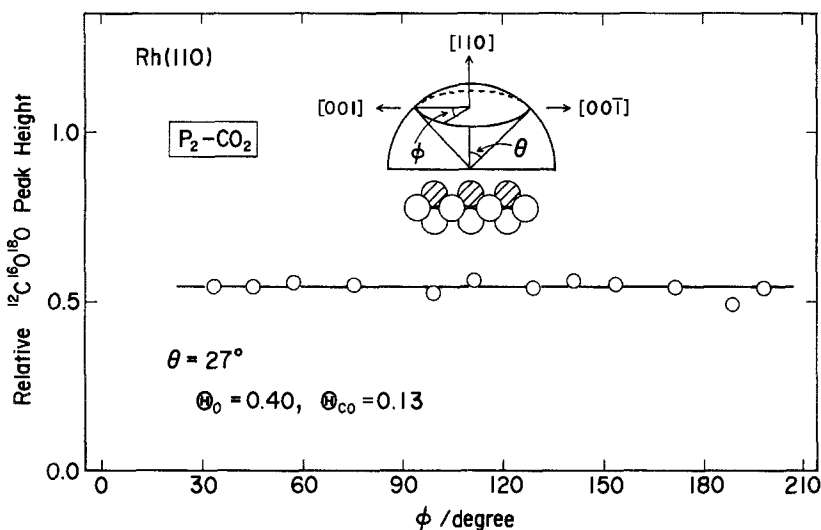


Fig. 5. Crystal azimuth dependence of the  $P_2$ -CO<sub>2</sub> flux at a fixed desorption angle of  $27^\circ$ . The experimental conditions are given in fig. 1.

## Acknowledgement

This work was partly supported by a Grant-in-Aid for General Scientific Research from the Ministry of Education, No. 03640419.

## References

- [1] T. Matsushima and H. Asada, *J. Chem. Phys.* 85 (1986) 1658.
- [2] T. Matsushima, *J. Chem. Phys.* 91 (1989) 5722;  
T. Matsushima, K. Shobatake, Y. Ohno and K. Tabayashi, *J. Chem. Phys.* 97 (1992) 2783.
- [3] T. Matsushima, *J. Chem. Phys.* 93 (1990) 1464;  
T. Matsushima, K. Shobatake and Y. Ohno, *Surf. Sci.* 283 (1993) 101.
- [4] T. Matsushima, Y. Ohno and K. Nagai, *J. Chem. Phys.* 94 (1991) 704.
- [5] M.A. Henderson, A. Szabo and J.T. Yates Jr., *J. Chem. Phys.* 91 (1989) 7245, 7255.
- [6] G. Comelli, V.R. Dhanak, M. Kiskinova, N. Pangher, G. Paolucci, K.C. Prince and R. Rosei, *Surf. Sci.* 260 (1992) 7;  
V.R. Dhanak, G. Comelli, G. Cautero, G. Paolucci, K.C. Prince, M. Kiskinova and R. Rosei, *Chem. Phys. Lett.* 188 (1992) 237.
- [7] E. Schwarz, J. Lenz, H. Wohlgemuth and K. Christmann, *Vacuum* 41 (1990) 167.
- [8] J.J. Weimer, J. Loboda-Cackovic and J.H. Block, *J. Vac. Sci. Technol. A* 8 (1990) 2543.
- [9] H. Conrad, G. Ertl and Küppers, *Surf. Sci.* 76 (1978) 323.
- [10] E.M. Stuve, R.J. Madix and C.R. Brundle, *Surf. Sci.* 146 (1984) 155.
- [11] Y. Ohno, T. Matsushima, K. Shobatake and H. Nozoye, *Surf. Sci.* 273 (1992) 291.
- [12] J.E. Reutt-Robey, D.J. Doren, Y.J. Chabal and S.B. Christman, *Phys. Rev. Lett.* 61 (1988) 2778.
- [13] F. Jensen, F. Besenbacher, E. Laegsgaard and I. Stensgaard, *Phys. Rev. B* 41 (1990) 10233.
- [14] D.J. Coulman, J. Winterlin, R.J. Behm and G. Ertl, *Phys. Rev. Lett.* 64 (1990) 1761.
- [15] M. Taniguchi, K. Tanaka, T. Hashizume and T. Sakurai, *Surf. Sci.* 262 (1992) L123.
- [16] M. Bowker, Q. Guo and R. Joyner, *Surf. Sci.* 253 (1991) 33.